ELSEVIER

Chemical Engineering Journal 139 (2008) 469–474

Chemical Engineering Journal

www.elsevier.com/locate/cej

A pilot investigation on oxidation of ammonium sulfite by streamer corona plasma

Xiaotu Hu [a,*], Tianle Zhu [b], Xuedong Jiang [a], Yi Wang [a], Ruichang Qiu [a], Hongdi Zhang [c], Ruinian Li [c], Keping Yan [d]

[a] *School of Electrical Engineering, Beijing Jiaotong University, Beijing 100044, China*
[b] *Department of Environmental Engineering, Beihang University, Beijing 100083, China*
[c] *Guangdong J-Tech Environment Science Co. Ltd., Guangzhou 510630, China*
[d] *Department of Environmental Science, Zhejiang University, Hangzhou 310028, China*

Received 14 January 2006; received in revised form 11 December 2006; accepted 9 August 2007

Abstract

For ammonia flue gas desulfurization (FGD), the sulfite to sulfate oxidation is very critical for industrial applications. This paper reports a novel corona plasma-induced oxidation technique to convert concentrated ammonium sulfites to sulfates in an aqueous solution. The streamer corona plasmas are generated with a dc superimposed ac power source. Ammonium sulfite solution is sprayed in a reactor by using two-phase nozzles. When the sulfite concentration is around 1–3 mol L^{-1}, the oxidation efficiency after one-cycle processing is in the range of 20–60%. Multiple-cycle treatments can be used to improve the oxidation efficiency. The energy consumption is around 20 Wh mol^{-1}. Based on the present investigations, we anticipate that an industrial plasma-assisted ammonium FGD can be applied in industries.
© 2007 Elsevier B.V. All rights reserved.

Keywords: Streamer corona; Flue gas desulfurization (FGD); Ammonium FGD; Sulfite oxidation; Plasma catalysis

1. Introduction

Ammonia-based FGD is a well-known technique. In 1935, Johnstone [1] reported its related thermodynamics via NH_3–SO_2–H_2O solution, which outlines the basic principle of almost all current ammonium FGDs. For electric power industries, the technique has hardly been used due to its costs. For chemical industries, however, it has been widely applied, where the intermediate byproduct of ammonium sulfite is often oxidized to ammonium sulfate. For example, in Ferrao and Bishoff process [2], about 8–10% of the sulfite is converted to sulfate in the scrubber, and around 80–90% of sulfites is oxidized in a separate reactor by O_2.

In literature, most reported work on the sulfite oxidation is related to atmospheric chemistry to explain the acid rain, where its solution concentration is in the order of a few mmol L^{-1} [3,4]. The related oxidation rate is too slow to be applied in industries. For example, under pH 5.0 and a temperature of 25 °C, the first-order rate constant is in the range of 1×10^{-5} to 2.5×10^{-4} s^{-1} for Na_2SO_3 solution [5]. For the stirred cell and packed column reactor reported by Li and his co-workers [6,7], their shortest observed characteristic time to reach 50% of sulfite oxidation in air is 15 min, where the sulfite concentration is around 0.3–0.4 mol L^{-1} and the Co^{2+} catalyst concentration is 0.4 mmol L^{-1}. For a high concentration of 2.58 mol L^{-1}, the characteristic time increases to 4 h. The reaction rate greatly drops when sulfite concentration increases. As a result, one may easily conclude that it would be too difficult to develop any cost-effective techniques based on air-induced oxidation of sulfites.

In the past 20 years, non-thermal plasma-induced desulfurization and denitrification process has been widely investigated in order to develop the so-called next generation zero emission technique [8–11]. Li et al. [11] reported that for corona plasma-assisted ammonium FGD, the produced salt whiskers play a very important role for sulfite oxidation. The generated OH radicals together with SO_2, O_2 and NH_3 are diffused into the liquid phase to initiate a series of chain reactions. As a result, tetravalent sulfocompounds S(IV) are oxidized to hexavalent ones S(VI). The molecular energy consumption can be as low as 3 eV/SO_2. The

* Corresponding author. Tel.: +86 10 51687121; fax: +86 10 51687121.
E-mail address: scuthxt@vip.sina.com (X. Hu).

1385-8947/$ – see front matter © 2007 Elsevier B.V. All rights reserved.
doi:10.1016/j.cej.2007.08.019

model is based on a hypothesis that the ammonium sulfate in the liquid phase is saturated.

In wet ammonium FGD process, the main reactions are shown in the following:

(1) SO_2 is absorbed by NH_3 into solution:

$$SO_2 + 2NH_3 + H_2O \rightarrow (NH_4)_2SO_3 \quad (1)$$

$$SO_2 + (NH_4)_2SO_3 + H_2O \rightarrow 2NH_4HSO_3 \quad (2)$$

$$NH_3 + NH_4HSO_3 \rightarrow (NH_4)_2SO_3 \quad (3)$$

(2) Ammonium sulfite oxidization:

$$2(NH_4)_2SO_3 + O_2 \rightarrow 2(NH_4)_2SO_4 \quad (4)$$

$$2NH_4HSO_3 + O_2 \rightarrow 2NH_4HSO_4 \quad (5)$$

This paper reports a novel corona plasma-induced ammonium sulfite oxidization technique to convert S(IV) to S(VI) in aqueous solutions, namely, the objective of oxidation process is to convert ammonium sulfite $(NH_4)_2SO_3$ and NH_4HSO_3 to ammonium sulfate $(NH_4)_2SO_4$ and NH_4HSO_4. The final product is solid form of $(NH_4)_2SO_4$ for agriculture fertilizer via NH_3 neutralization reaction and dry process. This oxidation technique is a critical step for the previously described semi-wet process ammonium FGD [12]. The main reactions are as follows:

$$2(NH_4)_2SO_3 + O_2 \xrightarrow{OH,O,O_3,HO_2,e} 2(NH_4)_2SO_4 \quad (6)$$

$$2NH_4HSO_3 + O_2 \xrightarrow{OH,O,O_3,HO_2,e} 2NH_4HSO_4 \quad (7)$$

The plasma-induced liquid-phase ammonium sulfite oxidization reactions are very complicated. They are a series of radical chain reactions in acidic aqueous solution [13,14]:

(1) Chain initiation:

$$OH^\bullet + HSO_3^- \rightarrow SO_3^{\bullet-} + H_2O \quad (8)$$

$$e_{aq} + H^+ \rightarrow H \quad (9)$$

$$H + O_2 \rightarrow HO_2^\bullet \quad (10)$$

$$HO_2^\bullet + HSO_3^- \rightarrow HSO_4^- + OH^\bullet \quad (11)$$

$$HO_2^\bullet + HSO_3^- \rightarrow SO_3^{\bullet-} + H_2O_2 \quad (12)$$

(2) Chain propagation:

$$SO_3^{\bullet-} + O_2 \cdot H_2O \rightarrow SO_5^{\bullet-} + H_2O \quad (13)$$

$$SO_5^{\bullet-} + SO_3^{2-} \rightarrow SO_4^{2-} + SO_4^{\bullet-} \quad (14)$$

$$SO_5^{\bullet-} + SO_3^{2-} \rightarrow SO_5^{2-} + SO_3^{\bullet-} \quad (15)$$

$$SO_5^{\bullet-} + HSO_3^- \rightarrow HSO_4^- + SO_4^{\bullet-} \quad (16)$$

$$SO_5^{\bullet-} + HSO_3^- \rightarrow HSO_5^- + SO_3^{\bullet-} \quad (17)$$

$$SO_4^{\bullet-} + HSO_3^- \rightarrow HSO_4^- + SO_3^{\bullet-} \quad (18)$$

$$SO_5^{\bullet-} + SO_5^{\bullet-} \rightarrow 2SO_4^{\bullet-} + O_2 \quad (19)$$

(3) Chain termination:

$$SO_3^{\bullet-} + SO_3^{\bullet-} \rightarrow S_2O_6^{2-} \quad (20)$$

$$SO_5^{\bullet-} + SO_5^{\bullet-} \rightarrow S_2O_8^{2-} + O_2 \quad (21)$$

$$SO_5^{\bullet-} + O_2^{\bullet-} \rightarrow SO_5^{2-} + O_2 \quad (22)$$

$$SO_5^{\bullet-} + HO_2 \rightarrow HSO_5^- + O_2 \quad (23)$$

$$HO_2^\bullet + HO_2^\bullet \rightarrow H_2O_2 + O_2 \quad (24)$$

$$HO_2 + O_2^{\bullet-} \rightarrow HO_2^- + O_2 \quad (25)$$

2. Experimental set-up

Fig. 1 shows the schematic diagram of the experimental set-up. A multi-channel wire-plate type corona reactor is used with a total volume of about 1 m^3. The geometry of anode electrode is saw-tooth wire, and the cathode electrode is plate, as shown in Fig. 2 . The plate–plate distance is in the range of 100–200 mm with a total length of the corona wire of 50–200 m. On the top of the reactor, multiple two-phase nozzles are installed to atomize the solution into the reactor. The sulfite solution from the container is firstly pumped to the atomizer and then sprayed into the reactor via compressed air. That is not only to atomize the solution, but also to provide oxygen for the oxidation.

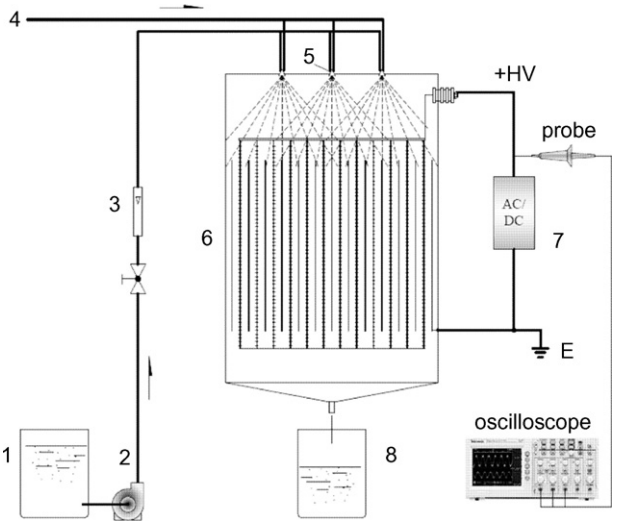

Fig. 1. Flowchart of experimental set-up: (1) sulfite solution container; (2) pump; (3) flowmeter; (4) compressed air; (5) nozzles; (6) plasma reactor; (7) ac/dc power supply; (8) byproduct container.

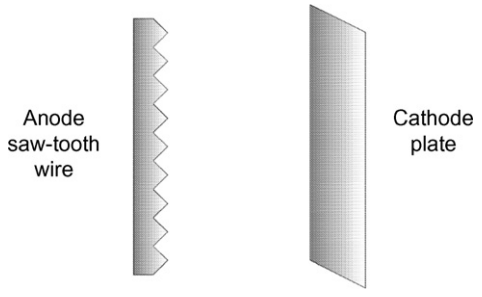

Fig. 2. The electrode geometry of plasma reactor.

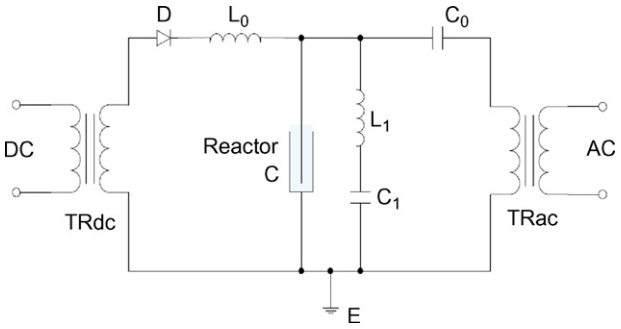

Fig. 3. Schematic circuit diagram of the dc/ac power source: TRdc, transformer in dc; TRac, transformer in ac; D, high-voltage diode; C, reactor; L_0, ac decoupling air-core inductor; C_0, high-voltage coupling capacitor; L_1, resonant inductor; C_1, resonant capacitor.

After the plasma-induced oxidation, the solution drops to a second container placed at the bottom of the reactor. And one-cycle treatment is performed.

As we know, positive streamer corona can lead to a good chemical efficiency. Using positive dc power source, however, can have a problem of generation of uniform streamer corona in a large plasma reactor [15]. In this work, we use a so-called dc/ac power source to energize the reactor [16]. Fig. 3 shows the circuit diagram. The dc/ac source mainly consists of two parts, namely a positive dc source and a high-frequency ac one. They are coupled together via a capacitor. For the present set-up, the dc applied voltage is from 10 to 35 kV; ac frequency is from 10 to 35 kHz, and the ac peak–peak voltage is up to 20 kV. Electrical measurements are carried out with a Tektronix TDS3014 oscilloscope. All used power consumption in this paper is referred to the input power from the mains. To show the plasma generation inside the reactor, Fig. 4 gives a streamer corona photo with saw-tooth type electrode.

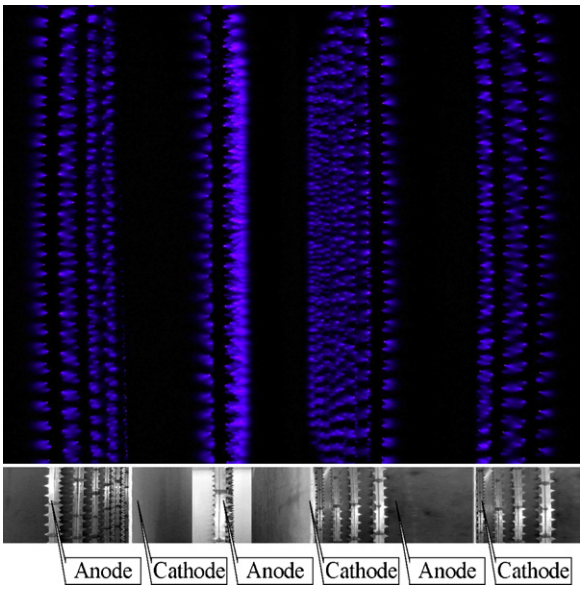

Fig. 4. A time integral picture of streamer discharges in a multi-channel saw-tooth wire-plate reactor.

The used sulfite solution is prepared via industrial ammonium sulfite with the compositions of 91.86% of $(NH_4)_2SO_3{\cdot}H_2O$, 0.14% of NH_4HSO_3, 4.70% of $(NH_4)_2SO_4$, and 3.30% of H_2O. Sulfite ions, namely SO_3^{2-} and HSO_3^-, are titrated in iodine solution by using dextrin solution as an indicator. The method mainly consists of the following two steps. Sulfites SO_3^{2-} and HSO_3^- are firstly oxidized by excessive iodine and then are titrated back with sodium thiosulfate. Details of the method are reported in the national standard [17]. The measurement of weights of sulfites and sulfates are also performed via the following two steps. After the sulfites are totally oxidized with iodine, the total sulfates are then precipitated with barium acetate. The precipitate is then filtered out, dried up, scorched and weighed in order to calculate the total weight [18].

3. Results and discussions

3.1. Spontaneous and plasma-induced oxidations

In order to distinguish the effects of spontaneous oxidation from the plasma-induced oxidation, experiments are performed by switching on and off plasma and at the same time to evaluate the sulfite oxidation. Fig. 5 gives a series of experimental results of one-cycle oxidation efficiency. Two series experiments are performed by using the same solution and under the same experimental conditions. Without producing plasma inside the reactor, the spontaneous oxidation rate is no more than 0.02 mol min^{-1}. When applying plasma, however, the oxidation rate can be as high as 0.35 mol min^{-1}. Plasma-induced oxidation is much faster than the air-initiated spontaneous oxidation.

3.2. Effects of sulfite concentration

In terms of oxidation efficiency, oxidation rate, energy consumption and the initial sulfite concentration, Figs. 6–8 show typical results of the effects of initial sulfite concentration on the process. All results are obtained after one-cycle processing. Experiments are carried out with the plate–plate distance of 200 mm, and under the solution temperature of 20 °C, the

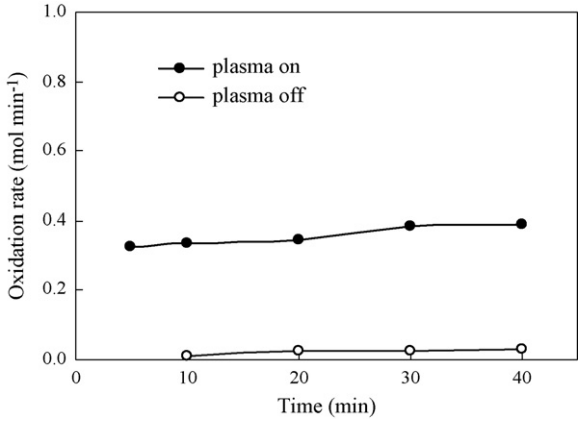

Fig. 5. Spontaneous and plasma-induced sulfite oxidation under the plate–plate gap distance of 100 mm, temperature of 20 °C, initial sulfite concentration of 1 mol L^{-1} and volumetric flow rate of the solution of 50 L h^{-1}.

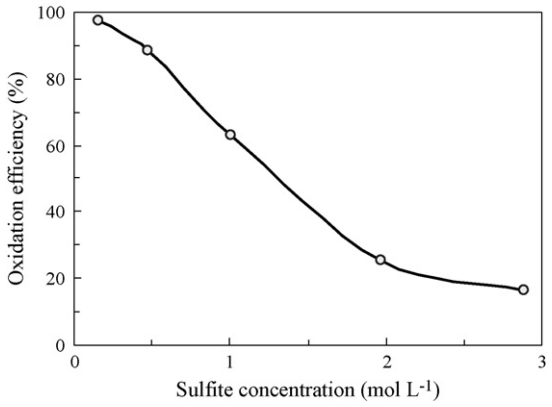

Fig. 6. Effects of the initial $(NH_4)_2SO_3$ concentration on the oxidation efficiency.

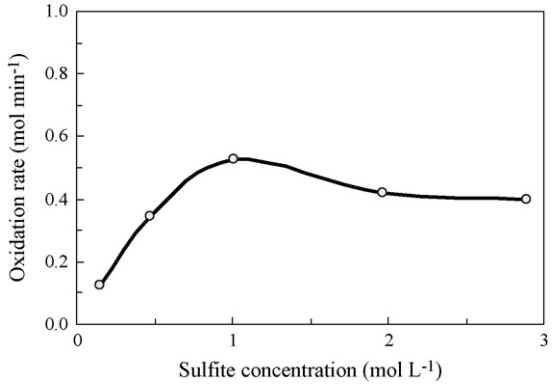

Fig. 7. Oxidation rate of $(NH_4)_2SO_3$ against the initial concentration.

solution flow rate of 50 L h^{-1}. Within the present tests with a concentration of 1–3 mol L^{-1}, the oxidation efficiency drops with the increase of the concentration. The observed efficiency and oxidation rate are much higher than that observed with an air-bubbling reactor. As an example, under the concentration of 1 mol L^{-1}, the efficiency and rate are about 60% and 0.5 mol min^{-1}, respectively, which are almost two orders of magnitude higher than that obtained with a direct air contact reactor [6,7].

With regard to the oxidation rate presented in Fig. 7, and the energy consumption indicated in Fig. 8, it seems that the

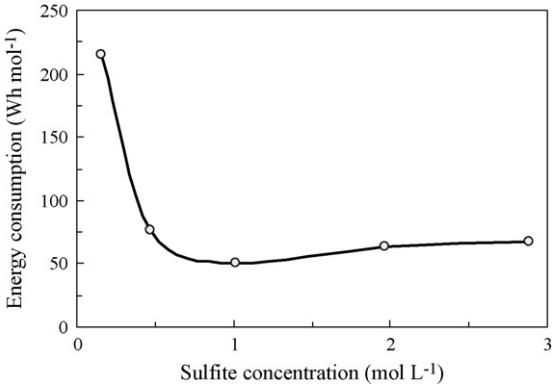

Fig. 8. Molar energy consumption against the initial $(NH_4)_2SO_3$ concentration.

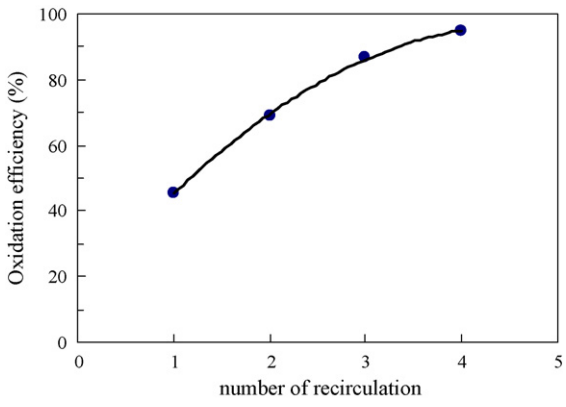

Fig. 9. Oxidation efficiency of $(NH_4)_2SO_3$ against the number of circulation. Multi-cycle treatment with a plate–plate gap distance of 200 mm and under the temperature of 20 °C, initial $(NH_4)_2SO_3$ concentration of 1.0 mol L^{-1}, solution flow rate of 50 L h^{-1}, and applied power of 1.4 kW.

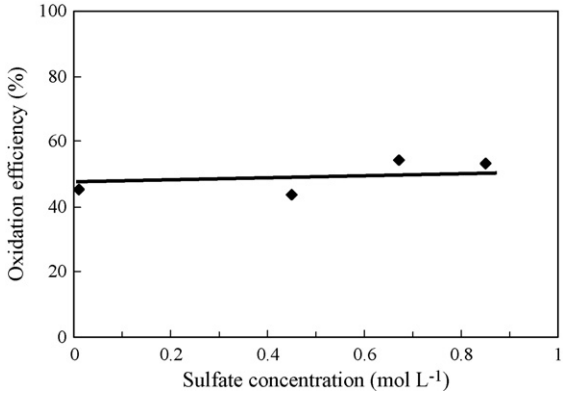

Fig. 10. Effects of sulfate $(NH_4)_2SO_4$ concentration on the oxidation efficiency of $(NH_4)_2SO_3$ under the following conditions: total concentration of 1 mol L^{-1} the flow rate of 50 L h^{-1}, the gap distance of 200 mm, temperature of 20 °C and applied power of 1.2 Wh.

plasma-induced oxidation process can be divided into two reaction regions by the initial concentration of around 1 mol L^{-1}. For a concentration of lower than 1 mol L^{-1}, the reaction rate increase and energy consumption drops when increasing the concentration. For the solution with a concentration of higher than 1 mol L^{-1}, both of them tend to reach stationary values. At

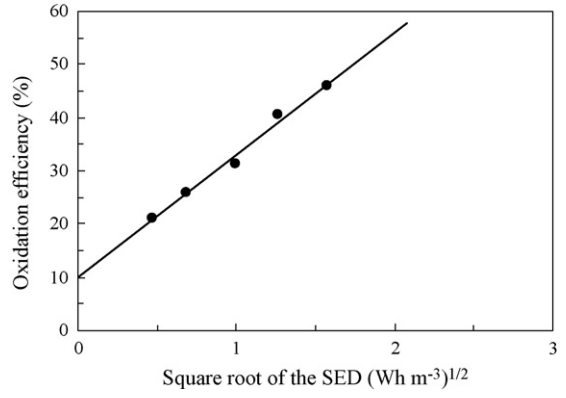

Fig. 11. Dependence of the oxidation efficiency on the square root of the corona specific energy density.

Table 1
Effects of treatment cycle on the oxidization rate and energy consumption

	Number of circulation			
	1	2	3	4
$(NH_4)_2SO_3$ oxidation rate of each cycle (mol h^{-1})	22.5	12.0	8.0	4.0
Energy consumption (Wh mol^{-1})	62	116	175	350

the concentration 1 mol L^{-1}, the molar energy consumption is around 50 Wh mol^{-1}, which is equivalent to a molecular energy consumption of 1.9 eV/S(IV). By converting the mole energy consumption of the ammonium sulfite oxidation to the specific energy density (SED) for 1000 ppm SO_2 removal from flue gas 50 Wh mol^{-1} is equivalent to 2.2 Wh Nm^{-3}. We also observed that the energy consumption depends on a number of experimental parameters, such as corona plasma power density, the reactor geometry, and the flow rate of compressed air. By optimizing these processing parameters, the minimum energy consumption for the present set-up is about 20 Wh mol^{-1}, which is equivalent to a molecular energy consumption of 0.75 eV/S(IV), corresponding the SED of 0.9 Wh Nm^{-3} for 1000 ppm SO_2 removal from flue gas and the SO_2 removal energy efficiency of 3.2 kg $(kWh)^{-1}$. In comparison with the other large scale pilot plant test results by using corona discharge plasma process, it is higher than those Dinelli et al. [19] and Wu et al. [20] reported, but lower than those Chang et al. [21] reported. Though it is too far for us to understand the oxidation process, there is at least one factor that can significantly affect the process, namely the O_2 solubility. As one expected, when increasing the initial concentration, the oxidation rate would increase. This seems true when the concentration is lower than 1 mol L^{-1}. It is also known that with increasing the concentration, the O_2 solubility decreases. As a result, the reaction rate will be decreased. According to the present investigations, we can conclude that in order to make the technique industrially applicable, the oxidation process has to be carried out under the initial sulfite concentration of not less than 3 mol L^{-1}.

3.3. Plasma-induced multiple-cycle treatment

In order to achieve higher oxidation efficiency, the solution can be repeatedly atomized into the reactor. Plasma-induced multiple-cycle treatment is then performed to oxidize the sulfite. Fig. 9 shows a typical result under an initial concentration of 1 mol L^{-1}. After the first, second, third and fourth cycles, the oxidation efficiencies are 45.4%, 68.9%, 86.9% and 93%, respectively. After four-cycle treatment, the oxidation efficiency is improved by a factor of 2. The energy consumption, unfortunately, is significantly increased. And the oxidation rate also greatly drops as listed in Table 1.

3.4. Effects of sulfate concentration

As a typical example, Fig. 10 plots the one-cycle oxidation efficiency of ammonium sulfite in terms of mole fraction of ammonium sulfate. For these experiments, the total concentration of sulfite and sulfate is equal to 1 mol L^{-1}. In contrast to the result presented in Fig. 6, where the oxidation efficiency increases with decreasing the sulfite concentration, the oxidation efficiency seems to keep a constant. Obviously, one can conclude that the co-existence of sulfate seems to negatively affect the oxidation. Considering the results shown in Figs. 6 and 10, one can also conclude that the efficiency of sulfite oxidation is dependent on the total concentration of both sulfites and sulfates.

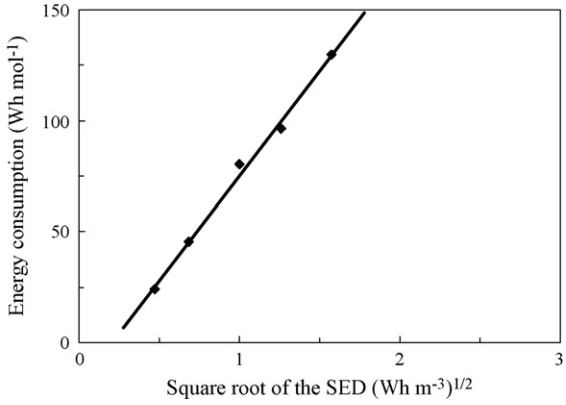

Fig. 12. Dependence of the molar energy consumption on the square root of the corona specific energy density.

3.5. Effects of plasma power density

Both oxidation efficiency and energy consumption are important indices for promoting industrial applications. Figs. 11 and 12 show typical experimental results for the first cycle oxidation under the initial concentration of 0.93 mol L^{-1} and a solution flow rate of 50 L h^{-1}. Under the present experimental conditions, convert the solution flow rate to a flow rate of flue gas with 1000 ppm SO_2 removed, we observed that both the oxidation efficiency and the molar energy consumption are linearly dependent on the square root of the corona specific energy density (SED), which is defined as the ratio of the average corona power to the gas flow rate. This observation is in agreement with early reported results [11]. Radical–radical termination reactions seem dominated the process.

4. Conclusion

Non-thermal plasmas can generate with either electron beam or corona discharge. In order to avoid the product adherent problem of dry ammonium in FGD process, a semi-wet or wet process is adopted. That differs from the electron beam and the other

corona discharge plasmas process. The mid-product, ammonium sulfite solution, in the wet technological process must be oxidized to sulfate as final products for agriculture fertilizer. Based on our pilot industrial experiments of ammonium sulfite oxidation, we can give the following remarks:

(1) In contrast to the plasma-induced oxidation, the spontaneous oxidations give negligible contributions to convert sulfite to sulfate. When the initial sulfite concentration is within 1–3 mol L^{-1}, plasma-induced one-cycle oxidation efficiency is in the range of 20–60%. Multiple-cycle treatment can be used to improve the efficiency under a cost of increasing the energy consumption.
(2) In terms of the initial $(NH_4)_2SO_3$ concentration, the plasma-induced oxidation process seemingly shows two different regions. When the concentration is around 1 mol L^{-1}, and the energy consumption is around 50 Wh mol^{-1}.
(3) To make the technique industrial applicable, the plasma-induced oxidation process should be performed under the initial concentration of not less than 3 mol L^{-1}.

Acknowledgement

The authors are indebted to Chinese National Department of Science and Technology, the Department of Science and Technology of Guangdong Province, and Guangzhou Bureau of Science and Technology for their supports via a national 863 project.

References

[1] H.F. Johnstone, Recovery of sulfur dioxide from waste gases, equilibrium partial vapor pressures over solutions of the ammonia–sulfur dioxide–water system, Ind. Eng. Chem. 27 (5) (1935) 587–593.
[2] F. Lourenco, Lentjes Bischoff ammonia water process for SO_2 absorption from flue gas, Chem. Eng. World 33 (11) (1998) 75–78.
[3] C. Brant, R. van Eldik, Transition metal-catalyzed oxidation of sulfur(IV) oxides, atmospheric-relevant processes and mechanisms, Chem. Rev. 95 (1) (1995) 119–177.
[4] V. Linek, V. Vacek, Chemical engineering use of catalyzed sulfite oxidation kinetics for the determination of mass transfer characteristics of gas–liquid contactors, Chem. Eng. Sci. 36 (11) (1981) 1747–1768.
[5] A.G. Clarke, M. Radojevic, Chloride ion effects on the aqueous oxidation of SO_2, Atmos. Environ. 17 (3) (1983) 617–624.
[6] W. Li, J. Zhou, W. Xiao, Oxidation of concentrated ammonium sulfite, J. East China Univ. Sci. Technol. 27 (3) (2001) 226–229.
[7] J. Zhou, W. Li, W. Xiao, Kinetics of heterogeneous oxidation of concentrated ammonium sulfite, Chem. Eng. Sci. (2000) 55.
[8] A. Mizuno, J.S. Clements, R.H. Davis, A method for the removal of sulfur dioxide from exhaust gas utilizing pulsed streamer corona for electron energization, IEEE Trans. Ind. Appl. IA-22 (3) (1986) 516–522.
[9] S. Masuda, H. Nakao, Control of NOx by positive and negative pulsed corona discharge, IEEE Trans./IA 26 (2) (1990) 374–383.
[10] S. Masuda, Report on novel dry $DeNO_x/DeSO_x$ technology for cleaning combustion gases from utility thermal power plant boilers, in: B.M. Penetrante, S.E. Schultheis (Eds.), In Non-thermal Plasma Techniques for Pollution Control: Part B, Springer-Verlag, Berlin, 1993.
[11] R. Li, K. Yan, J. Mao, X. Wu, Heterogeneous reactions in non-thermal plasma flue gas desulfurization, Chem. Eng. Sci. 53 (8) (1998) 1529–1540.
[12] K. Yan, R. Li, T. Zhu, H. Zhang, X. Hu, X. Jiang, H. Liang, R. Qiu, Y. Wang, A semi-wet technological process for flue gas desulfurization by corona discharges at an industrial scale, Chem. Eng. J. 116 (2006) 139–147.
[13] R.E. Huie, P. Neta, Rate constants for some oxidations of S(IV) by radicals in aqueous solutions, Atmos. Environ. 21 (8) (1987) 1743–1747.
[14] A.N. Ermakov, G.A. Poskrebyshev, A.P. Purmal, Sulfite oxidation: the state-of-the-art of the problem, Kinet. Catal. 38 (3) (1997) 295–308.
[15] K. Yan, Corona plasma generation, Ph.D. Thesis, Eindhoven University of Technology, Eindhoven, The Netherlands, 2001, pp. 9–11 (ISBN: 90-386-1870-0).
[16] K. Yan, T. Yamamoto, S. Kanazawa, T. Ohkubo, Y. Nomoto, J.S. Chang, NO removal characteristics of a corona radical shower system under DC and AC/DC superimposed operations, IEEE Trans. Ind. Applic. 37 (5) (2001) 1499–1504.
[17] State environmental protection administration of China, HJ/T 56-2000, Determination of sulphur dioxide from exhausted gas of stationary source. Iodine titration method, 2000.
[18] T. Zhou, E. Wang, W. Lu, Analytical Chemistry Handbook. Part 2. Chemical Analysis, Chemical Industry Press, Beijing, China, 1997, p. 36.
[19] G. Dinelli, L. Civitano, M. Rea, Industrial experiments on pulse corona simultaneous removal of NOx and SO_2 from flue gas, IEEE Trans. Ind. Appl. 25 (1990) 535–541.
[20] Y. Wu, N. Wang, Y. Zhu, Y. Zhang, SO_2 removal from industrial flue gases using pulsed corona discharge, J. Electrostat. 44 (1998) 11–16.
[21] J.S. Chang, K. Urashima, Y.X. Tong, W.P. Liu, H.Y. Wei, F.M. Yang, X.J. Liu, Simultaneous removal of NOx and SO_2 from coal boiler flue gases by DC corona discharge ammonia radical shower systems: pilot plant tests, J. Electrostat. 57 (2003) 313–323.